Enhanced Binding of a Rationally Designed Peptide Ligand of Concanavalin A Arises from Improved Geometrical Complementarity†

Deepti Jain, Kanwal J. Kaur, and Dinakar M. Salunke*

Structural Biology Unit, National Institute of Immunology, Aruna Asaf Ali Marg, New Delhi 110 067, India

Received June 18, 2001; Revised Manuscript Received August 2, 2001

ABSTRACT: The structural basis of affinity enhancement was addressed by analyzing the interactions between concanavalin A and the carbohydrate-mimicking peptide ligands. Based on the crystal structures of concanavalin A in complex with these peptides [Jain, D., Kaur, K. J., Sundaravadivel, B., and Salunke, D. M. (2000) *J. Biol. Chem. 275*, 16098−16102; Jain, D., Kaur, K. J., and Salunke, D. M. (2001) *Biophys. J. 80*, 2912−2921], a high-affinity analogue was designed. This analogue (acetyl-MYWYPY-amide) binds to the lectin with 32-fold enhanced affinity compared to the corresponding precursor peptides. The crystal structure of concanavalin A bound to the designed peptide has been determined. A peptide molecule binds to each of the crystallographically independent monomers of the tetrameric lectin. The four bound peptide molecules exhibit two major conformations both of which are extended. Unlike in the case of other concanavalin A binding peptides, the structural variations within different conformers of this analogue are marginal. It is apparent that the deletion of the structurally variable region of the larger peptides has led to an improved complementarity and increased buried surface area in the case of the designed peptide. The crystal structure also showed the formation of two backbone hydrogen bonds between the ligand and the ligate which were not present in the complexes of the precursor peptides. The observed structural features adequately explain the enhanced binding of the designed analogue.

Specificity and affinity are critical parameters associated with molecular interactions influencing umpteen biological processes. Molecular design studies in the context of drug discovery primarily focus on the optimization of specificity and affinity of a ligand to the corresponding target receptor. Establishing the direct correlation of these parameters with structural features is an essential component of drug design applications. Many elaborate studies have been carried out addressing structural and mechanistic aspects of ligand−receptor recognition with regard to delineation of the determinants of specificity and affinity (*1*−*5*). However, the present structural understanding of molecular recognition is constantly evolving while exposing the complexity of structural design that facilitates specific interactions. The conformational flexibility—of the ligand as well as the receptor (*6*)—and the ability of solvent molecules to act as cementing factor (*7*) play an important role in optimizing specificity and affinity. The traditional approaches involving random screening have led to a number of ligands being picked up, but the elegant optimization is best carried out on the basis of structural studies.

The comparative structural analysis involving two rationally designed analogues of the carbohydrate-mimicking peptides in terms of their interactions with concanavalin A (ConA)[1] explaining their differential affinities is the focus of the present study. ConA, a lectin from *Canavalia ensiformis*, has been extensively exploited for understanding protein−carbohydrate recognition (*8*−*13*) and addressing the structural basis of molecular mimicry (*14*, *15*). Several peptides bind to ConA with affinities comparable to that of methyl α-D-mannopyranoside (89 μM), a well-characterized carbohydrate ligand of ConA (*16*, *17*). A possible topological equivalence was suggested between the 12mer (DVFYPY-PYASGS) peptide and methyl α-D-mannopyranoside since the binding of sugar to ConA could be competitively inhibited by peptide in a dose-dependent manner and the polyclonal antibodies against one cross-reacted with the other (*14*). Crystallographic analysis of the 12mer−ConA complex revealed the structural relationship between peptide and carbohydrate moiety in terms of surface topology and their interactions with ConA (*15*, *18*).

The crystal structures of 15mer (RVWYPYGSYLTASGS), 10mer (MYWYPYASGS), and 12mer complexed with ConA facilitated delineation of the residues defining specificity (*6*), on the one hand, and the associated conformational plasticity in different environments in ConA−peptide recognition, on the other. The extent of plasticity in the peptide conformation and interactions could be due to the relatively weak binding to ConA. The wealth of information regarding molecular interactions in the three crystal structures involving related peptides provided rationale for designing a higher affinity peptide analogue. This paper reports the design and the

† This work was supported by the Department of Biotechnology (GOI) with funds provided to the National Institute of Immunology. D.J. is the recipient of a fellowship from the CSIR (India).

* Correspondence should be addressed to this author at the Structural Biology Unit, National Institute of Immunology, Aruna Asaf Ali Marg, New Delhi 110 067, India. FAX: 91 11 616 2125; Phone: 91 11 616 7623, ext. 234; E-mail: dinakar@nii.res.in.

[1] Abbreviations: ConA, concanavalin A; rms, root-mean-square; Ac, acetyl.

10.1021/bi011254f CCC: $20.00
Published on Web 09/13/2001

crystal structure analysis of such an analogue complexed with ConA. The structure reveals that the enhanced affinity of the designed peptide is a result of truncation of the conformationally variable region of the parent peptide, which improves the complementarity of surfaces when bound to ConA.

EXPERIMENTAL PROCEDURES

Peptide Synthesis and Purification. The 15mer, 12mer, and 10mer peptides were synthesized on an automated peptide synthesizer (Applied Biosystems, model 431A) using solid-phase 9-fluorenylmethyloxycarbonyl (Fmoc) chemistry, as described earlier (*14*). For synthesis of capped-6mer, rink amide resin (Nova Biochem) was used. After completion of synthesis and removal of the Fmoc group, the resin was treated with acetic anhydride/triethylamine/dimethylformamide (1:1:8) to acetylate the terminal amino group. Cleavage was performed using trifluoroacetic acid/1,2-ethanedithiol/H_2O (9.5:0.25:0.25). The crude peptides were purified on a Waters Deltapak reverse-phase C18 100 Å (19 × 300 mm, 15 μm, spherical) column on a preparative HPLC (Waters) using a linear gradient of water and acetonitrile. The absorption was monitored at 214 nm. Characterization was performed by molecular mass determination using a single-quadruple mass analyzer (Fisons Instruments, U.K.).

ConA Binding Assay. The 12mer was conjugated to BSA using glutaraldehyde as described earlier (*14*). 12mer−BSA conjugate (1 μg/well) was absorbed onto 96 well Maxisorb Nunc plates in 50 mM sodium carbonate buffer, pH 9.6, overnight at 4 °C. Wells with absorbed antigens were blocked with 1% bovine serum albumin. Plates were incubated for 1.5 h at 37 °C with constant amounts of biotinylated ConA and equal volumes of increasing amounts of the peptides. The ConA binding was detected by streptavidin−peroxidase. As a control, wells coated with the antigen and incubated with streptavidin−peroxidase without lectin were used. The level of inhibition was calculated by comparison of the absorbance at 490 nm of the wells reacted with ConA with and without the soluble inhibitor. Results were calculated from duplicate measurements.

Crystallization and Data Collection. Cocrystallization of ConA (Sigma) at a concentration of 0.32 mM with peptide (20-fold molar excess) was carried out using the hanging drop method. The crystals were obtained using ammonium sulfate at pH 9.0 in 50 mM Tris buffer. Methanol was added in order to increase the solubility of the peptide. The X-ray intensity data for ConA−peptide complex crystals were collected on an Image Plate detector (Marresearch, Germany) installed on a rotating anode X-ray source (RIGAKU, Japan). The diffraction data were collected at a crystal to detector distance of 235 mm, with 0.25° oscillation frames up to 3.0 Å resolution from two different crystals, processed separately using DENZO (*19*), and subsequently merged using SCALEPACK. The space group symmetry is $C222_1$.

Structure Determination and Refinement. The dimer of the tetrameric ConA in complex with methyl α-D-mannopyranoside (5CNA) (*20*) was used as a probe model for molecular replacement using AMoRe (*21*) between 8 and 4 Å resolution. The solution was unambiguous and showed the presence of two dimers within the asymmetric unit. The initial model was subjected to rigid-body refinement in X-PLOR. Initially, dimer was treated as a rigid body, and subsequently each monomer was treated independently. The individual atoms were then refined by several cycles of conventional positional refinement with overall *B* values. Both conventional *R*-factor (R_{cryst}) and the free *R*-value (R_{free}), using 5% data (*22*), were used to monitor the progress of refinement. CNS (*23*) was used in the later stages of refinement. Some of the loops of the ConA model were rebuilt in electron density and were displayed with the help of O (*24*) on O2 (Silicon Graphics Inc.). Noncrystallographic symmetry restraints with a weight of 120 kcal mol^{-1} $Å^{-2}$ were used for ConA throughout the refinement. The parameter and topology files used in CNS were modified to include specifications for the N-terminal acetyl and C-terminal amide group. These groups were added to the 6′mer peptide, and the complete structure was refined followed by iterative building of the peptide model on the basis of $2F_o-F_c$ and F_o-F_c maps (*25*). Water molecules were included in the model using an electron density cutoff of 2.5σ in F_o-F_c and 1σ in $2F_o-F_c$ and if they were within 3.5 Å from one or more nitrogen or oxygen atoms of the protein or other water molecule. The final coordinates and the structure factor data have been deposited in the protein data bank (PDB code: 1JOJ).

Analysis and Comparison of Models. The deviation from ideal geometry of the ConA−peptide complex was analyzed using PROCHECK (*26*) in CCP4. The buried surface area (i.e., the area rendered inaccessible to a 1.4 Å sphere) of each residue in the complex was determined using the HOMOLOGY module of MSI (Biosystems) installed on Octane (Silicon Graphics Inc.). The CONTACT program of the CCP4 package was used to determine van der Waals contacts and hydrogen bonds between peptide and ConA. The structures were compared on the basis of root-mean-square (rms) deviation of the ConA backbone and the peptide conformers within the asymmetric unit. The superimposition of structures was carried out using InsightII (Biosystems). The shape complementarity coefficient, S_c, was calculated using the Lawrence and Colman method where a coefficient of 1 on the scale of 0−1 indicates maximum complementarity between the two surfaces (*27*). For the 10mer conformers, the values were calculated for first six residues and for the designed analogue; the S_c values were calculated by removing the acetate and the amide groups from the peptide.

RESULTS

Design of Higher Affinity Peptide Ligand. It is evident that the carbohydrate-mimicking peptides, 15mer, 12mer, and 10mer, as seen from the structures of their complexes with ConA, exhibit maximum interactions with the protein through the N-terminal region (*6*, *18*). The carboxyl-terminal Ala-Ser-Gly-Ser segment shows significant structural variations and fewer interactions with ConA (Figure 1). Therefore, the deletion of C-terminal residues may improve the affinity of the peptide for ConA. Moreover, the consensus motif Tyr-Pro-Tyr, in the family of phage display selected sequences, forms the hydrophobic framework for ConA interactions and provides specificity for ConA−peptide recognition. It is clear that this motif is critical for the design of any new peptide with enhanced affinity. However, the 6mer (MYWYPY), which does not have the carboxyl-terminal four residues Ala-Ser-Gly-Ser, binds to ConA with much weaker affinity than that of 15mer, 12mer, and 10mer (*14*, *17*).

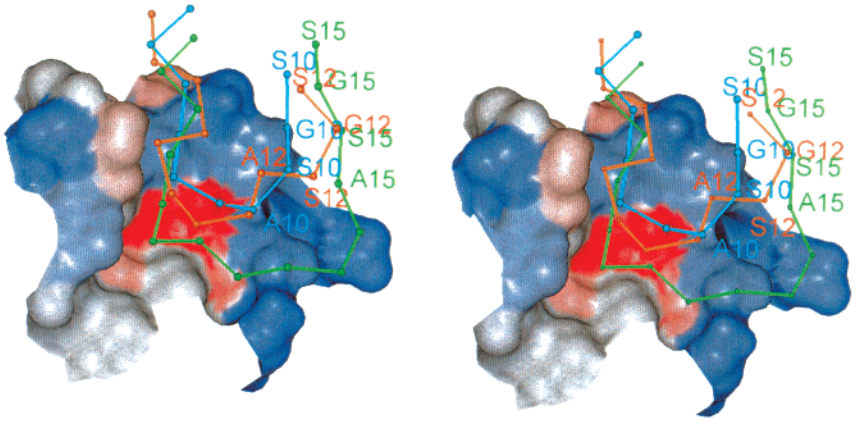

FIGURE 1: Stereoscopic view of the superimposition of the peptides bound to the A subunit of ConA in three different crystal structures. Interactions of the three peptides (drawn in Cα-trace, ball-and-stick) with the corresponding ConA residues within 4 Å distance of the peptides. The 15mer, 10mer, and 12mer are shown in green, cyan, and orange colors, respectively. The Ala-Ser-Gly-Ser segments of the peptides are labeled in corresponding colors, and ConA is represented as surface decorated with hydropathy features where blue and red correspond to hydrophilic and hydrophobic regions, respectively.

It is apparent that the binding of 10mer is primarily facilitated by interactions of the N-terminal region of the peptide. In this context, weak binding of 6mer is intriguing. The plausible reason for this anomaly could be that the presence of a negatively charged terminal carboxylate group of 6mer is unfavorable in the relatively nonpolar environment on the corresponding subsite of ConA. Shifting of this group, as in the case of 10mer, further away to interact with the solvent may be facilitating its binding to ConA. Therefore, a peptide was designed where the amino and carboxyl ends of the 6mer were capped with acetyl and amide groups, respectively, obtaining the analogue 6′mer (Ac-MYWYPY-amide).

The binding of this peptide to ConA was tested in a competitive assay and compared with the earlier known peptide ligands of ConA. The results indicated that all the peptides bind to ConA in a dose-dependent manner. Whereas the free 6mer does not show any detectable binding within the concentration range tested, the 6′mer binds to ConA with about 32-fold higher affinity with respect to 10mer (Figure 2). The IC_{30} values for the designed analogue and the 10mer were 0.06 and 1.9 mM, respectively. Thus, to investigate the structural correlates of enhanced binding of the truncated peptide with blocked ends, the crystallographic studies of 6′mer were carried out in complex with ConA.

Overall Structure. The ConA−6′mer complex is isomorphous to the other ConA−peptide complexes described earlier (*6*, *18*). The asymmetric unit consists of two dimers, AB and CD, whose structures are identical. The four independent ConA monomers are bound to four peptide molecules (P, Q, R, and S). Figure 3 represents the F_o-F_c electron density map of one of the four conformations of the 6′mer. The crystal structure has been refined to R_{cryst} of 18.6% and R_{free} of 23.1%. The refinement statistics are outlined in Table 1. The final model of ConA in complex with 6′mer consists of 237 residues of ConA, 2 metal ions (Mg^{2+} and Ca^{2+}) and a peptide molecule in each of the 4 monomers, and 198 solvent molecules. The three-dimensional structure of ConA in complex with 6′mer resembles the other peptide-bound forms. The main chains of the four ConA subunits within the asymmetric unit superimpose on each other with rms deviations that lie within 0.37 Å,

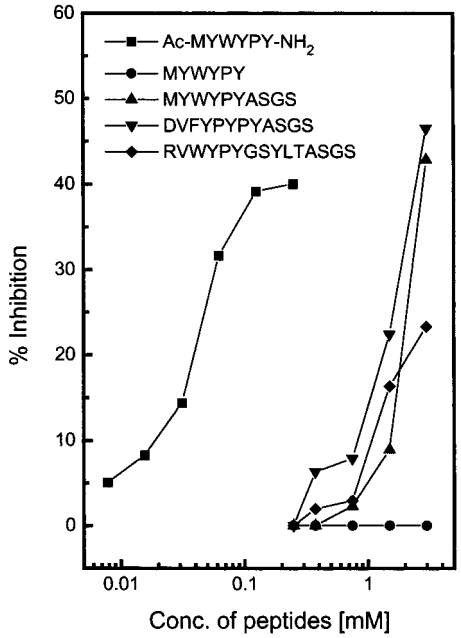

FIGURE 2: Inhibition of ConA binding to solid-phase 12mer−BSA by soluble 6′mer. Biotinylated ConA at a concentration of 4 μg/mL was incubated with an increasing amount of different peptides, and binding of free biotinylated lectin to absorbed 12mer−BSA was measured using peroxidase-labeled streptavidin. The range of the peptide concentrations analyzed is limited by the corresponding solubilities.

demonstrating the absence of major structural changes, although some local conformational differences in the side chain orientations were observed. Additionally, the peptide binding loop, including residues 200−206, also shows certain differences between A and B subunits. The rms deviation for this loop between A and B subunits for Cα atoms is 0.93 Å and is lowest among all the complexes (*6*, *18*).

Peptide Conformation. All the residues of the peptide molecules (P, Q, R, S) bound to the four subunits of ConA were unambiguously identified in the ConA−6′mer complex. The main chain of 6′mer shows an extended conformation in all four cases with no standard secondary structural elements. The conformational data of the S conformer are listed in Table 2. Superimposition of the four 6′mer conformers is shown in Figure 4A. The conformers P and S

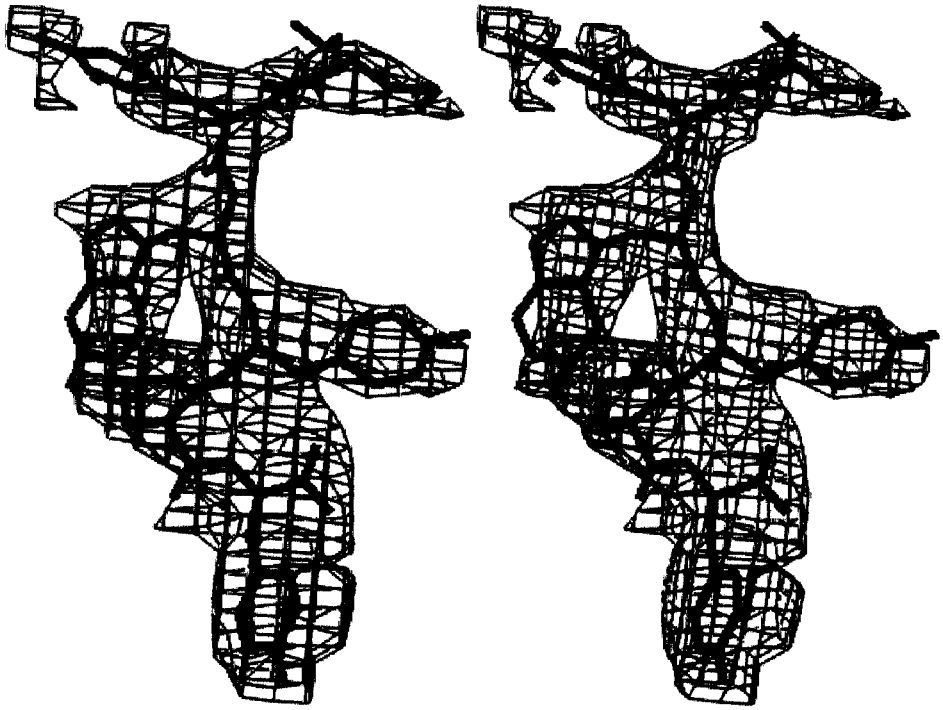

FIGURE 3: Stereoscopic view of the F_o-F_c difference electron density map of 6′mer bound to ConA.

Table 1: Crystal Data and Refinement Statistics of ConA in Complex with 6′mer

ligand	Ac-MYWYPY-amide
cell constants (Å)	$a = 102.68$; $b = 118.38$; $c = 253.59$
space group	$C222_1$
maximum resolution (Å)[a]	3.0
completeness (%)	78.1 (71.8)[b]
no. of independent reflections	23957
multiplicity	3
average $I/\sigma I$	10.6 (5.37)
R_{merge} (%)	10.1 (25.7)
no. of protein atoms	7236
no. of peptide atoms	276
no. of ions	8
no. of solvent atoms	198
rms deviation bond length (Å)	0.008
rms deviation bond angles (deg)	1.688
R_{cryst} (%)	18.6
R_{free} (%)	23.1
B factor, overall (Å^2)	20.92

[a] The true resolution is 3.1 Å. [b] The values in parentheses are for the last resolution shell between 3 and 3.13 Å.

Table 2: Torsion Angles (deg) of *S* Conformer of 6′mer

	φ	ψ	$\chi1$	$\chi2$	$\chi3$
M2	−127.2	65.9	−170.6	60.5	127.6
Y3	−125.4	139.9	51.3	46.8	
W4	−145.9	−18.6	46.7	−153.8	
Y5	−162.9	144.2	70.7	162.0	
P6	−78.9	−68.5			
Y7	−123.8	77.0	−51.5	59.4	

display an rms deviation of 1.29 Å, and Q and R conformers are almost identical with an rms deviation of 0.13 Å.

The conformational correlations of the 6′mer can be explained on the basis of crystal environment. The molecular packing in the crystals is such that the symmetry environment of P and Q is similar to that of S and R conformers, respectively. The peptide conformations in the P and S environments are relatively solvent-exposed and are free from symmetry interactions. On the other hand, the symmetry environments of Q and R are such that the peptides interact with symmetry-related ConA molecules. Thus, the structural variations in the peptide conformations between the conformers bound at equivalent symmetry position are less due to deletion of the noninteracting variable region of the peptide. However, the rms deviations between the peptides bound at nonequivalent symmetry environments, P (and S) and Q (and R), are of the order of 1.2 Å.

Interactions of the Peptide with ConA. The four independent peptide molecules bind at the same site in all four subunits in a shallow cleft on the surface of the protein. Almost all the residues of the peptide in the case of 6′mer interact with ConA. A total of 12 different residues of the protein are involved in interactions with peptide when all the subunits are considered together. Met1 of P and Ac and amide groups of S do not show interactions at all. The amino acid residues of ConA that are involved in van der Waals interactions with each residue of the bound peptide in all four conformations are listed in Table 3. The P and S conformers interact with symmetry-related ConA through Tyr6 as well as with symmetry-related peptide through Pro5, Tyr6, and the amide group. Thus, in these two conformations, the peptide exhibits contacts with only one residue of the symmetry-related ConA. The P and S conformers exhibit eight and four hydrogen bonds with ConA, respectively. The W3:N and W3:O of the P conformer forms backbone hydrogen bonds with N44A:O and N44A:N of ConA, respectively. The S conformer shows only one backbone hydrogen bond between W3:O and N44:N. The other hydrogen bonds are formed involving the side chain atoms. Upon formation of the complex, 411 and 330 Å^2 solvent-accessible area of P and S conformations becomes buried, respectively (Table 4).

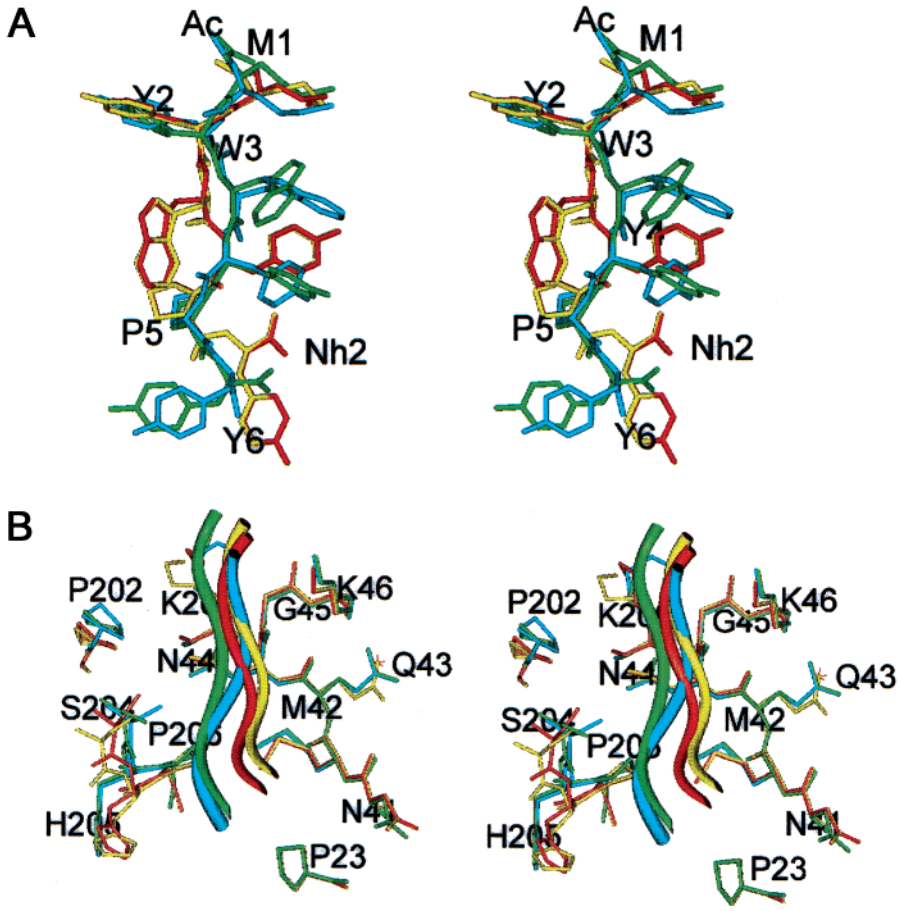

FIGURE 4: Stereoscopic view of the comparison of the 6′mer conformers and their interactions within the asymmetric unit. (A) Least-squares superimposition of the peptide conformers P, Q, R, and S. (B) The four ConA subunits along with their respective bound peptides (drawn as ribbons) are superimposed. Only the interacting residues of ConA within 4 Å distance of the ligand are shown in each case. The P, Q, R, and S are colored in cyan, red, yellow, and green, respectively.

Table 3: van der Waals Contacts of Four Different Conformations of 6′mer

6′mer	P	S	Q	R
Ac	K46		K46	K46
M1		K46	K46	K46
Y2	N44		N44	
	G45		G45	G45
	K46			
	K200	K200	K200	K200
		P202		
W3	Q43		Q43	Q43
	N44	N44	N44	N44
		G45		
		K46		
			S204	S204
Y4	N41			
	M42		Q43	Q43
		N44		N44
	S204	S204		
P5			M42	M42
				Q43
	N44	N44	N44	N44
	S204	S204		
	P206	P206		
Y6	P23			
	H205	H205		
amide	P23			

Q and R bind to B and C subunits of ConA, respectively, and are sandwiched between two crystallographically related molecules. The peptide forms direct interatomic contacts with ConA through the Ac group to Pro5 and shows extensive interactions with subunits that are crystallographically related. The C-terminal Tyr6 and the amide group interact exclusively with symmetry-related peptide molecules. Q and R conformers are stabilized by interactions from the symmetry-related ConA molecules and hence are identical. However, 6′mer, being a smaller peptide, exhibits fewer symmetry interactions as compared to the other three ConA−peptide complexes (*6*, *18*). Q and R form five and four hydrogen bonds, respectively, with the corresponding subunit. The W3:N and W3:O of both conformers form backbone hydrogen bonds with N44:O and N44:N of the respective ConA subunit. The other hydrogen bonds involve side chain interactions. Upon formation of the complex, 343 and 281 Å^2 solvent-accessible area of the Q and R conformers becomes buried, respectively (Table 4). The detailed interactions of each conformation with its respective ConA subunit are depicted in Figure 4B.

Table 4: Comparison of the Buried Surface Area (BSA in Å^2) and Surface Complementarity Index (S_c) of 6′mer Conformers with the First Six Residues of 10mer

	6′mer			10mer		
conformer	$BSA_{peptide}$	BSA_{ConA}	S_c	$BSA_{peptide}$	BSA_{ConA}	S_c
P	411.83	320.13	0.669	231.49	234.34	0.609
Q	343.57	326.15	0.625	238.72	247.79	0.516
R	281.09	306.42	0.590	199.89	204.20	0.425
S	330.37	303.85	0.591	322.33	288.00	0.549

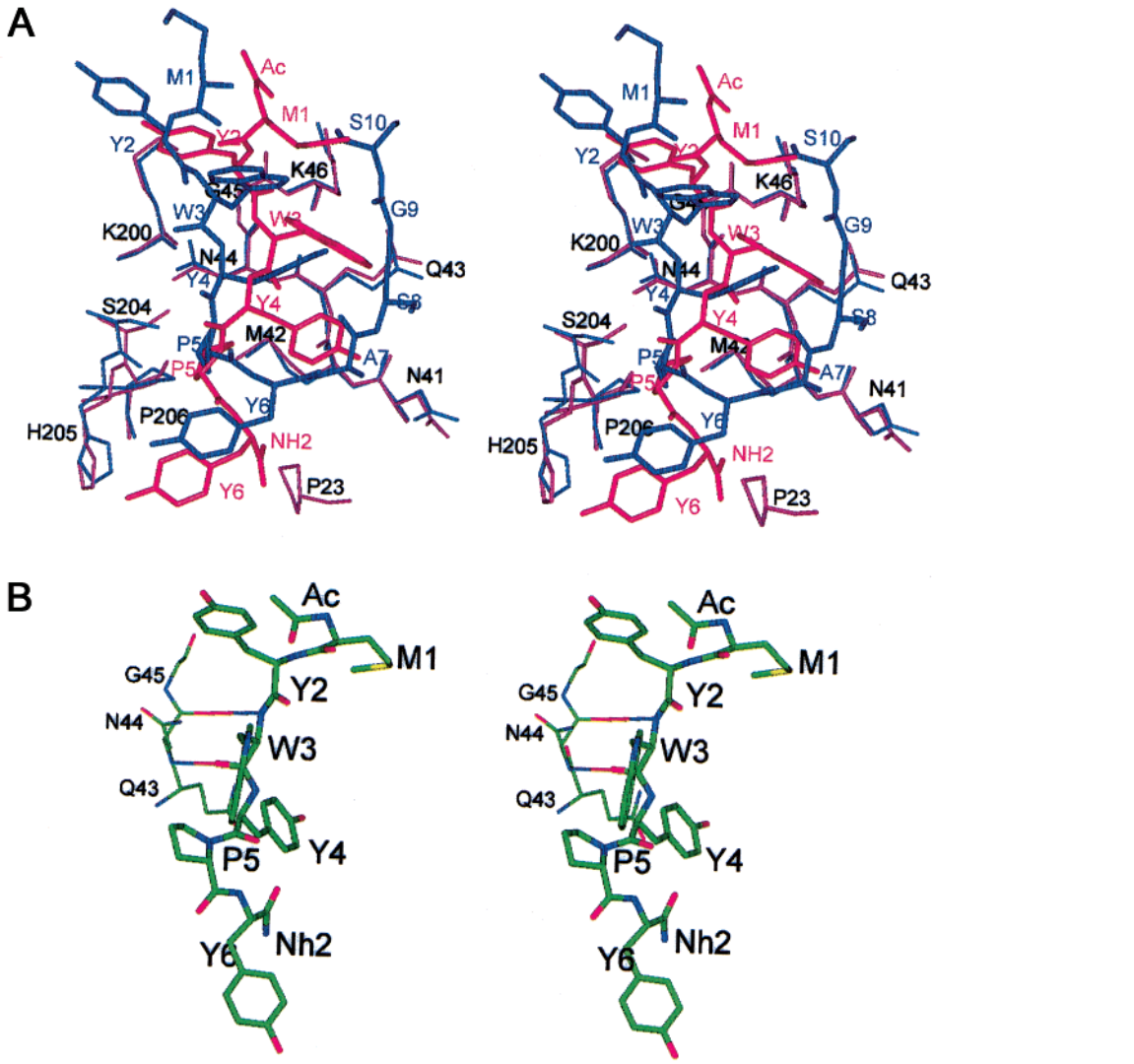

FIGURE 5: Stereoscopic view of the superimposition of the 10mer and 6′mer structures and interactions of the peptides bound to the A subunit of ConA. (A) Interactions of the two peptides (in stick) with the corresponding ConA residues within 4 Å distance of the peptides. The 10mer and 6′mer are shown in blue and magenta, respectively. (B) The backbone hydrogen bonds in 6′mer. The ConA and peptide residues are in thin and thick sticks, respectively.

Comparison between 6′mer and 10mer. As the peptide 6′mer shares N-terminal sequence with 10mer, it was relevant to compare the structures of these two peptides. The 10mer and the 6′mer bind and occupy approximately the same space within the binding cavity on ConA. The 10mer shows significant conformational variations while binding to ConA; however, these variations are more pronounced at the C-terminus of the peptide. Two of the four conformers that are solvent-exposed adopt a folded structure in the case of the 10mer. The other two have extended C-termini. On the other hand, in the case of the 6′mer, all four conformers have similar extended conformations, and those that are involved in symmetry interactions are identical.

Significant differences occur in the interactions of the two peptides with ConA (Figure 5A). The binding subsites for 6′mer were defined on ConA. Despite the similarity in sequence with 10mer, 6′mer shows contacts involving a different set of ConA residues for the Met1, Tyr2, and Trp3 of the peptide. On the other hand, both 10mer and 6′mer share the binding pocket of Tyr-Pro-Tyr, which includes residues Pro23, Asn41, Met42, Gln43, Asn44, Ser204, His205, and Pro206 of ConA. As shown earlier, this motif contributes toward the specificity of ConA−peptide interactions (*18*). The 6′mer has its ends capped with acetate and amide groups, which show additional interactions with ConA. These interactions are absent in the case of the 10mer. In three of the four conformers of 6′mer (P, Q, and R), the Ac:O of the peptide hydrogen bonds with Lys46:NZ. In the Q conformer, the amide group forms an end-to-end hydrogen bond with Y6:O of P. Comparison of the surface complementarity (S_c) index of the two peptides shows higher values for 6′mer conformers (0.59−0.66) compared to the corresponding residues in the 10mer conformers (0.42−60) (Table 4).

DISCUSSION

The structure-based rational design in the present study resulted in approximately 32-fold improvement in the affinity of the peptide. Our design of a peptide with enhanced affinity is based on the analyses of a series of crystal structures of peptide−ConA complexes. The randomized sequences on the surface of filamentous phages are often used to select ligands. However, these peptides have extremely variable affinities. The factors affecting the affinity in general have

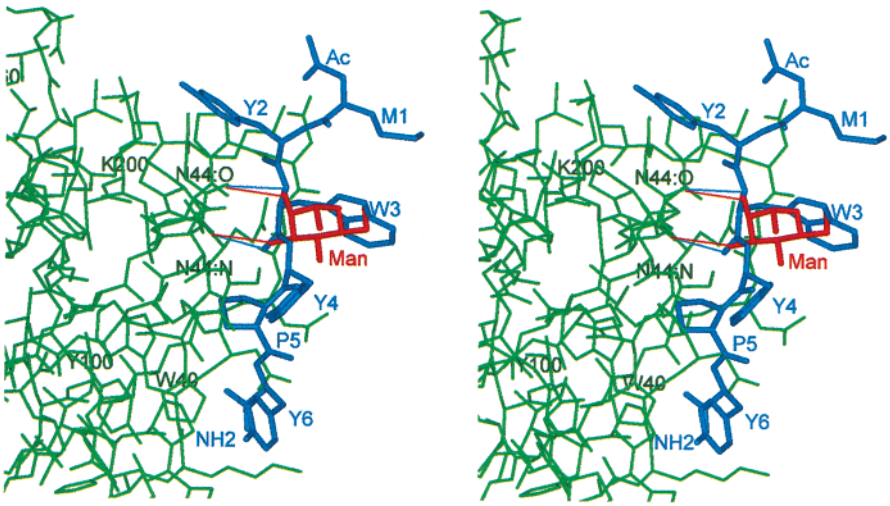

FIGURE 6: Stereoscopic view of the structural superimposition of methyl α-D-mannopyranoside in the 6′mer binding site on ConA optimized by overlap of the backbone hydrogen bonds of the 6′mer−ConA complex. A part of the ConA molecule incorporating the peptide binding site has been displayed with every 20th residue labeled. The ConA, peptide, and mannose are shown in green, blue, and red, respectively.

been addressed earlier. In several instances, the affinities of the ligands have been optimized by substitution mutagenesis (*4*, *28*, *29*) or by constraining the conformation of the ligand to reduce flexibility (*30*−*32*). In fact, the majority of the precursor peptides used, while designing the higher affinity 6′mer analogue, were derived from the phage display libraries.

Geometrical complementarity is essential in defining the specificity of recognition in diverse processes. Structural comparison between 10mer and 6′mer highlights some obvious differences, which evince direct correlation with the differential ConA binding of the two peptides. The total buried surface area of 6′mer is higher than that in the case of the corresponding residues of 10mer in all four independent conformers, resulting in improved complementarity with ConA. Surface complementarity, which is a commonly employed basis for optimization in many docking algorithms (*33*, *34*), represents the structural characteristics of the differential affinities of 10mer and 6′mer. It is evident that the 6′mer shows a significantly higher index for surface complementarity (S_c) as compared to corresponding residues in the 10mer. Three out of the four conformers of 6′mer make two hydrogen bonds through backbone atoms of the peptide as well as ConA (Figure 5B). The relatively higher binding of the 6′mer with respect to the other three peptides and the mannose moiety may be due to these hydrogen bonds since the backbone hydrogen bonds provide higher stability in protein structure and interactions. Such a contribution of hydrogen bonding and hydrophobicity between the ligand and the receptor has been demonstrated in other cases as well (*1*−*3*). The structural superimposition of methyl α-D-mannopyranoside in the 6′mer binding site on ConA suggests the possibility of similarity of hydrogen bonding interactions as seen from Figure 6. However, the number of van der Waals contacts shown by sugar is about one-tenth of those shown by the peptide. Thus, the collective contribution of backbone hydrogen bonding and geometrical complementarity appears to be critical for the relatively higher affinity of 6′mer.

The difference in the binding pattern of 6′mer with respect to the other carbohydrate-mimicking peptides can be correlated with two factors. First, the three peptides—15mer, 12mer, and 10mer—have extended C-terminal regions that impart more flexibility, leading to higher conformational entropy and hence lesser affinity. Truncation of the flexible four residue segment, that shows relatively fewer interactions with ConA, improves the complementarity of the peptide with ConA. Second, neutralization of the N-terminal and C-terminal regions with respect to free 6mer may also be responsible for the higher affinity of 6′mer since the protecting groups synergistically add to the stability of interactions.

Thus, the structural comparison presented here provides the basis of enhanced binding of the 6′mer in complex with ConA. The increase in the affinity of 6′mer to ConA can be attributed to increased surface complementarity, which in turn leads to better charge complementarity (as manifested in the appearance of new hydrogen bonds between the main chain of the peptide and that of ConA). Thus, 6′mer functions as the minimal effective peptide that binds to ConA with relatively higher affinity. Such structural details of the ligand−receptor recognition are important for deciphering the nature of their specificities, which has enormous implications in rational drug design. Our data may also be relevant in understanding the structural basis of affinity maturation of the antibodies which occurs through iterative somatic hypermutations such that the specificity is progressively enhanced. Other such specificity-dependent phenomena may also be dominated by similar structural factors.

REFERENCES

1. Weber, P. C., Ohlendorf, D. H., Wendoloski, J. J., and Salemme, F. R. (1989) *Science 243*, 85−88.
2. Rahuel, J., Garcia-Echeverria, C., Furet, P., Strauss, A., Caravatti, G., Fretz, H., Schoepfer, J., and Gay, B. (1998) *J. Mol. Biol. 279*, 1013−1022.
3. Nair, S. K., Krebs, J. F., Christianson, D. W., and Fierke, C. A. (1995) *Biochemistry 34*, 3981−3989.
4. Sharon, J. (1990) *Proc. Natl. Acad. Sci. U.S.A. 87*, 4814−4817.
5. Xu, J., Deng, Q., Chen, J., Houk, K. N., Bartek, J., Hilvert, D., and Wilson, I. (1999) *Science 286*, 2345−2348.
6. Jain, D., Kaur, K. J., and Salunke, D. M. (2001) *Biophys. J. 80*, 2912−2921.
7. Ravishankar, R., Ravindran, M., Saguna, K., Surolia, A., and Vijayan, M. (1997) *Curr. Sci. 72*, 855−861.

8. Derewenda, Z., Yariv, J., Helliwell, J. R., Kalb (Gilboa), A. J., Dodson, E. J., Papiz, M. Z., Wan, T., and Campbell, J. (1989) *EMBO J. 8*, 2189−2193.
9. Bradbrook, G. M., Gleichmann, T., Harrop, S. J., Habash, J., Raftery, J., Kalb (Gilboa), J., Yariv, J., Hillier, I. H., and Helliwell, J. R. (1998) *J. Chem. Soc., Faraday Trans. 94*, 1603−1611.
10. Bradbrook, G. M., Forshaw, J. R., and Perez, S. (2000) *Eur. J. Biochem. 267*, 4545−4555.
11. Naismith, J. H., and Field, R. A. (1996) *J. Biol. Chem. 271*, 972−976.
12. Loris, R., Maes, D., Poortmans, F., Wyns, L., and Bouckaert, J. (1996) *J. Biol. Chem. 271*, 30614−30618.
13. Moothoo, D. N., Canan, B., Field, R. A., and Naismith, J. H. (1999) *Glycobiology 9*, 539−545.
14. Kaur, K. J., Khurana, S., and Salunke, D. M. (1997) *J. Biol. Chem. 272*, 5539−5543.
15. Jain, D., Kaur, K., Goel, M., and Salunke, D. M. (2000) *Biochem. Biophys. Res. Commun. 272*, 843−849.
16. Oldenberg, K. R., Loganathan, D., Goldstein, I. J., Schultz, P. G., and Gallop, M. A. (1992) *Proc. Natl. Acad. Sci. U.S.A. 89*, 5393−5397.
17. Scott, J. K., Loganathan, D., Easly, R. B., Gong, X., and Goldstein, I. J. (1992) *Proc. Natl. Acad. Sci. U.S.A. 89*, 5398−5402.
18. Jain, D., Kaur, K. J., Sundaravadivel, B., and Salunke, D. M. (2000) *J. Biol. Chem. 275*, 16098−16102.
19. Otwinowski, Z. (1993) *Oscillation data reduction program*, pp 56−62, SERC Daresbury Laboratory, Warrington, U.K.
20. Naismith, J. H., Emmerich, C., Habash, J., Harrop, S. J., Helliwell, J. R., Hunter, W. N., Raftery, J., Kalb (Gilboa), A. J., and Yariv, J. (1994) *Acta Crystallogr., Sect. D D50*, 847−858.
21. Navaza, J. (1994) *Acta Crystallogr., Sect. A A50*, 157−163.
22. Brünger, A. T. (1992) *Nature 355*, 472−474.
23. Brünger, A. T., Adams, P. D., Clore, G. M., DeLano, W. L., Gros, P., Grosse-Kunstleve, R. W., Jian-Sheng, J., Kuszewski, J., Nilges, M., Pannu, N. S., Read, R. J., Rice, L. M., Simonson, T., and Warren, G. L. (1998) *Acta Crystallogr., Sect. D D54*, 905−921.
24. Jones, T. A., Cowan, S., Zou, J. Y., and Kjeldgaard, M. (1991) *Acta Crystallogr., Sect. A A47*, 110−119.
25. CCP4, SERC Daresbury Laboratory, Warrington, WA4 4AD, England. (1994) *Acta Crystallogr., Sect. D D50*, 760−763.
26. Laskowski, R. A., MacArthur, M. W., Moss, D. S., and Thornton, J. M. (1993) *J. Appl. Crystallogr. 26*, 238−291.
27. Lawrence, M. C., and Colman, P. M. (1993) *J. Mol. Biol. 234*, 946−950.
28. Chen, Y., Wiesmann, C., Fuh, G., Li, B., Christinger, H. W., McKay, P., de Vos, A. M., and Lowman, H. B. (1999) *J. Mol. Biol. 293*, 865−881.
29. Sainz, E., Akeson, M., Mantey, S. A., Jensen, R. T., and Battey, J. F. (1998) *J. Biol. Chem. 273*, 15927−15932.
30. Urban, J., Qabar, M., Sia, C., Klein, M., and Kahn, M. (1996) *Bioorg. Med. Chem. 4*, 673−676.
31. Cabezas, E., Wang, M., Parren, P. W. H. I., Stanfield, R. L., and Satterthwait, A. C. (2000) *Biochemistry 39*, 14377−14391.
32. Balass, M., Kalef, E., Fuchs, S., and Katchalski-Katzir, E. (2001) *Toxicon 39*, 1045−1051.
33. Sobolev, V., Wade, R. C., Vriend, G., and Edelman, M. (1996) *Proteins: Struct., Funct., Genet. 25*, 120−129.
34. Meyer, M., Wilson, P., and Schomburg, D. (1996) *J. Mol. Biol. 264*, 199−210.

BI011254F